

Hexaphenyl-1,2-Diphosphonium Dication $[\text{Ph}_3\text{P}-\text{PPh}_3]^{2+}$: Superacid, Superoxidant, or Super Reagent?

Fabian Dankert, Simon P. Muhm, Chandan Nandi, Sergi Danés, Sneha Mullassery, Petra Herbeck-Engel, Bernd Morgenstern, Robert Weiss,* Pedro Salvador,* and Dominik Munz*



Cite This: *J. Am. Chem. Soc.* 2025, 147, 15369–15376



Read Online

ACCESS |

Metrics & More

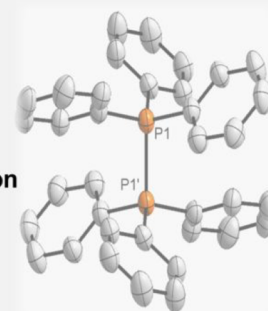
Article Recommendations

Supporting Information

ABSTRACT: The oxidation of triphenylphosphine by perfluorinated phenazinium^F aluminate in difluorobenzene affords hexaaryl-1,2-diphosphonium dialuminate **1**. Dication **1**²⁺ is valence isoelectronic with elusive hexaphenylethane, where instead the formation of a mixture of the trityl radical and Gomberg's dimer is favored. Quantum-chemical calculations in combination with Raman/IR spectroscopies rationalize the stability of the P–P bonded dimer in **1**²⁺ and suggest, akin to the halogens, facile homolytic as well as heterolytic scission. Thus, **1**²⁺ serves as a surrogate of both the triphenylphosphorandylum dication (Ph_3P^{2+}) and the triphenylphosphine radical monocation ($\text{Ph}_3\text{P}^{\cdot+}$). Treating **1** with dimethylaminopyridine (DMAP) or ^tBu₃P replaces triphenylphosphine under heterolytic P–P bond scission. Qualifying as a superoxidant (*E* vs Fc/Fc⁺ = +1.44 V), **1** oxidizes trimethylphosphine. Based on halide abstraction experiments (⁻BF₄, ⁻PF₆, ⁻SbCl₆, ⁻SbF₆) as well as the deoxygenation of triethylphosphine oxide, triflate anions as well as toluic acid, **1** also features Lewis superacidity. The controlled hydrolysis affords Hendrickson's reagent, which itself finds broad use as a dehydration agent. Formally, homolytic P–P bond scission occurs with diphenyldisulfide (PhSSPh) and the triple bonds in benzo- and acetonitrile. The irradiation by light cleaves the P–P bond homolytically and generates transient triphenylphosphine radical cations, which engage in H-atom abstraction as well as CH phosphorylation.

$[\text{Ph}_3\text{P}-\text{PPh}_3]^{2+}$

- ✓ Superacid, Superoxidant
- ✓ H- and O-Atom Abstraction
- ✓ Ph_3P^{2+} Transfer Reagent
- ✓ $\text{Ph}_3\text{P}^{\cdot+}$ Transfer Reagent
- ✓ sc-XRD, Raman, DFT



INTRODUCTION

In the quest for hexaphenylethane (Scheme 1, I), Moses Gomberg reported the triphenylmethyl (trityl) radical **II** in 1900.¹ The discovery of “trivalent carbon” is considered nowadays the beginning of organic radical chemistry. Later scrutiny revealed that the trityl radical had been obtained only in marginal yield, as it dimerizes instead through addition to the *para*-position of one phenyl substituent (Gomberg's dimer **III**).² Whereas heavier hexaphenylsilane is isolable,³ corresponding addition reactions to the *para*-position also occur for the valence isoelectronic triphenylboryl radical anion⁴ and the triphenylamine radical cation.⁵ In the 1970s, it was found that the decoration of the phenyl substituents shifts the equilibrium to respective hexaarylethane dimers.⁶ Phenyl group decoration similarly allows for a shift of the equilibrium toward monocationic triarylamine radical monomers⁷ and dianionic diboron(6) dimers.⁸ The adduct of triphenylphosphine with the trityl cation $[\text{Ph}_3\text{P}-\text{CPh}_3]^+$ is isolable, yet the isomer derived from *para*-addition is thermodynamically more stable.⁹

In stark contrast, both the hexaphenyl-1,2-diphosphonium dication as well as the triphenylphosphine radical cation remain elusive.¹⁰ Triphenylphosphine radical cations are

believed to serve as transient key intermediates in (photo)-redox catalysis,¹¹ as well as even arene hydrogenation by water.¹² It is known furthermore that the sterically encumbered trimesitylphosphine radical cation does not dimerize.¹³ This radical may be obtained in crystalline form upon treating (Mes)₃P with Al(C₆F₅)₃,^{13b} thus bridging the fields of Frustrated Lewis Pairs (FLPs)¹⁴ and radical chemistry.¹⁵ Another phosphine radical cation was stabilized thanks to three bulky halogenated naphthyl substituents, where the halogen atoms directly interact with the radical site.¹⁶ The treatment of red phosphorus by primary alkyl iodides¹⁷ as well as the permethylation of diphosphines R₂P–PR₂ by an excess of methyl triflate (R = Me) affords respective dimers, namely peraliphatic ⁺P–P⁺ vicinal diphosphonium dications.¹⁸ The $[\text{Me}_3\text{P}-\text{PMe}_3]^{2+}$ dication has been the subject of various studies, including its generation through oxidation of

Received: January 21, 2025

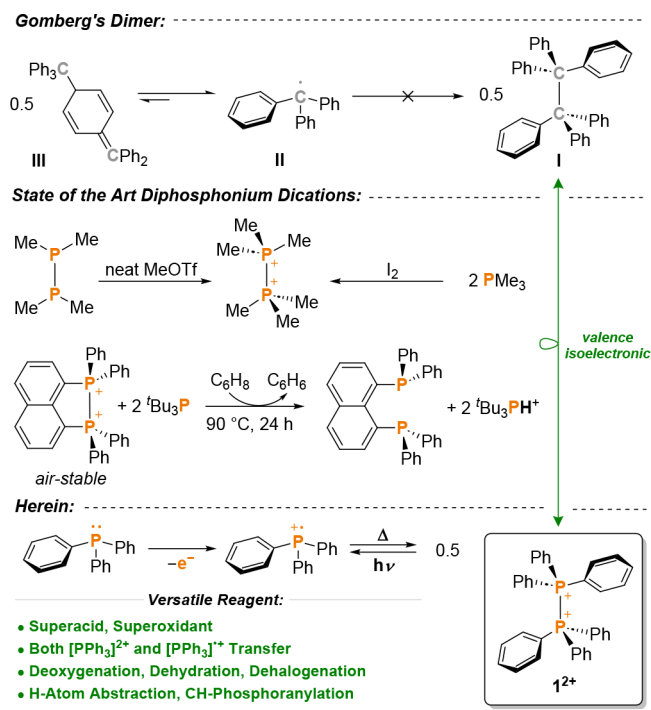
Revised: April 13, 2025

Accepted: April 14, 2025

Published: April 24, 2025



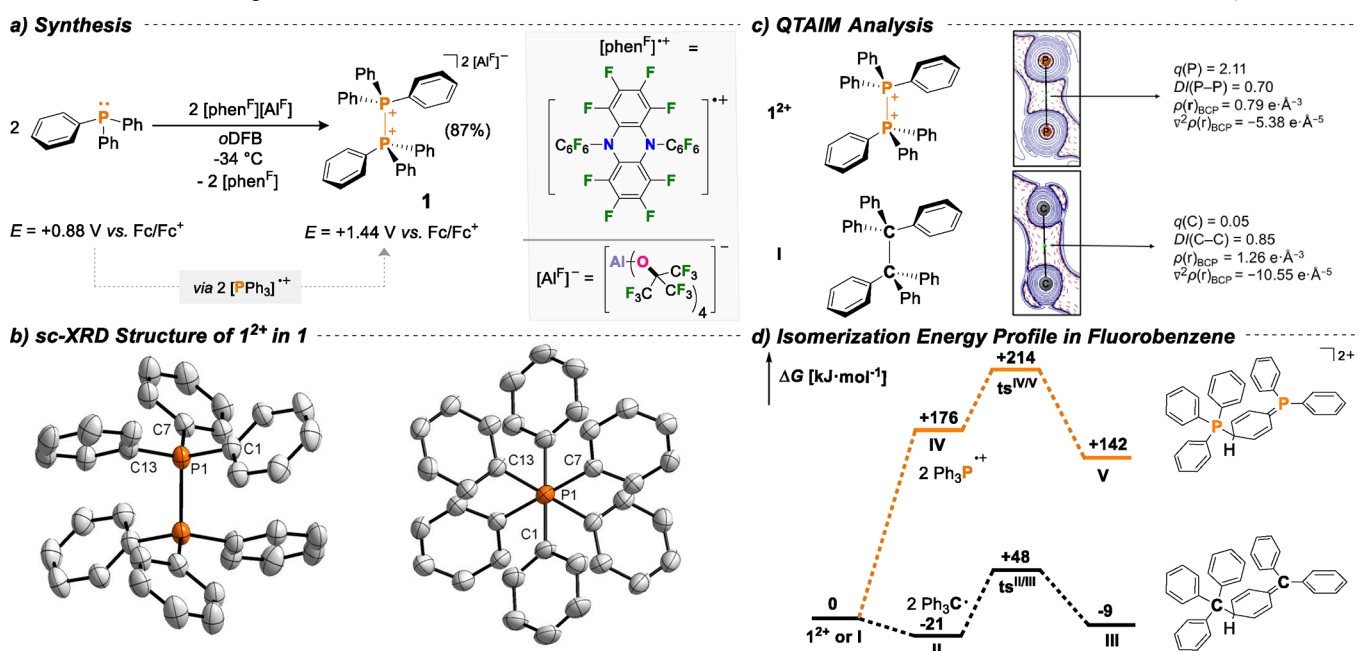
Scheme 1. Triphenylmethyl Radicals Associate to Gombert's Dimer (Top), yet the Isovalence Electronic Triphenylphosphine Radical Cation Affords the Hexaphenyl-1,2-diphosphonium Dication (Bottom)



pyrophoric PMe_3 by electrochemistry¹⁹ or iodine,²⁰ heavy group 15 oxidants such as $Sb(V)$,²¹ and copper(II)²⁰ complexes. The electronic structure of the unusual vicinal dicationic²² $+P-P^+$ bond has been investigated computationally and spectroscopically.²³ It has been argued (i) that the $+P-P^+$ bond is more susceptible to homolytic than heterolytic cleavage and (ii) that the vicinal cationic charges infer covalency. Although known since the 1980s and in stark contrast to transient triphenylphosphine radical cations (*vide supra*), these peraliphatic dications have not yet found application in catalysis or organic synthesis. It was reported, however, that they readily react with nucleophiles such as water, thiols, dipropyl disulfide, and secondary amines, yet not with aromatic CH bonds or olefins.^{19,24}

Enforcing two phosphorus centers into proximity by a rigid bridge represents an alternative approach to 1,2-diphosphonium dications.²⁵ Treating the naphthalene-linked P^V/P^{III} precursor $(Ph_2F_2P)(C_{10}H_6)(PPh_2)$ with the triethylsilylium cation afforded the respective $+P-P^+$ dication. This compound is persistent in the air and shows a moderate acceptor number (AN) of 30.²⁶ The addition of the Lewis base P^tBu_3 generates a powerful FLP of high hydridophilicity, as was demonstrated by hydride abstraction from triethylsilane (24 h, room temperature) and even the C–H dehydrogenation of cyclohexadiene (24 h, 90 °C). Encouraged by the bond-activation chemistry by formal phosphorus dications,²⁷ constrained phosphonium monocations,²⁸ the emergence of organopnictogen redox catalysis,²⁹ as well as reports on formal carbon dications,³⁰ we turned our attention toward oxidizing triphenylphosphine by an “innocent” oxidant. The fluorinated phenazinium radical

Scheme 2. (a) Synthesis of 1; (b) sc-XRD Structure of 1^{2+} in Single-Crystals of $1 \cdot C_6H_2F_4$; (c) QTAIM Analysis of 1^{2+} and I, Ph_3C-CPh_3 ; Blue Lines Indicate Charge Depletion ($\nabla^2\rho(r) > 0$), Red Dashed Lines Show Charge Concentration ($\nabla^2\rho(r) < 0$); the Solid Black Lines are Bond Paths, the Green Dots are Bond Critical Points (BCP); q_i Partial Charges; DI, Delocalization Indices; $\nabla^2\rho(r)_{BCP}$, Laplacian at the BCP; $\rho(r)_{BCP}$, Electron Density at the BCP; (d) Energy Profile for the Formation of Gombert's-dimer at the CPCM(PhF)-PBE0-D3/def2-TZVPP//PBE0-D3/def2-SVP Level of Theory^a



^aAnions and cocrystallized $C_6H_2F_4$ are omitted for clarity, thermal ellipsoids are given at 50% probability. Selected bond lengths [Å] and angles [°] in 1: P1–P1, 2.262(3); P1–C1, 1.794(4); P1–C7, 1.786(4); P1–C13, 1.794(4); C1–P1–C7, 111.5(2); C7–P1–C13, 113.2(2); C1–P1–C13, 112.2(2); C13–P1–P1, 105.8(2); C7–P1–P1, 106.6(2); C13–P1–P1, 105.8(2); C13–P1–P1–C13, 180°.

cations reported by the Crossing group appeared to be a promising choice,³¹ as they are prepared with aluminate anions.³² Here, we report that triphenylphosphine is swiftly oxidized by such “deelectronators”, thereby affording the hexaaryl-1,2-diphosphonium dication 1^{2+} . Spectroscopic as well as computational investigations rationalize the stability of 1^{2+} with respect to Gomberg’s dimer. Reactivity studies demonstrate (i) both homo- and heterolytic cleavage of the P–P bond, (ii) Lewis (super)acidity, (iii) H-atom abstraction capabilities, and (iv) that dication 1^{2+} serves as a powerful deoxygenation and phosphorylation agent.

RESULTS AND DISCUSSION

Treating triphenylphosphine in cold *ortho*-difluorobenzene (*o*DFB) or 1,2,3,4-tetrafluorobenzene (TFB) with two equivalents of [phen^F][Al^F] ([phen^F] = [perfluoro-5,10-bis(perfluorophenyl)-5,10-dihydrophenazinium]⁺; [Al^F] = [Al{OC(CF₃)₃}₄][−]) or [ant^{Cl,F}][Al^F] (see SI) afforded a faint yellow solution (Scheme 2a). A crystalline, colorless precipitate formed upon slow warming of the solution to room temperature. The precipitate was identified as **1** according to the ³¹P NMR spectroscopic analysis with a signal at 17.6 ppm (c.f. [Me₃P–PMe₃][OTf]₂ 28.4 ppm),¹⁸ and was isolated in 87% crystalline yield after workup. Compound **1** is thermally robust, with decomposition starting around +260 °C (Figure S18). Single-crystal X-ray diffraction (sc-XRD) confirmed the formation of hexaphenyl-1,2-diphosphonium dialuminate [Ph₃P–PPh₃][Al^F]₂ (**1**, Scheme 2b). In the solid-state structure, an inversion center is found between the two phosphorus atoms, which implies a staggered conformation of the phenyl groups. Although the crystallographic data are of moderate quality (see SI for details), they enabled the determination of reasonably reliable structural metrics for the dication in **1**. The P–P bond of 2.262(3) Å is elongated in comparison to the PMe₃-congener (2.198(2) Å).¹⁸ The comparison with triphenylphosphine reveals that the P–C bonds in **1** are shorter (**1**, 1.794(4), 1.786(4), 1.794(4) Å; PPh₃, ~1.823 Å) and that the C–P–C angles (**1**, 111.5(2), 113.2(2), 112.2(2)°; PPh₃, ~102°) are larger, thus indicating significant planarization and charge-delocalization.

The Raman (IR, respectively; Figures S15–S17) vibrational spectroscopy revealed bands at $\tilde{\nu} = 191$ and 611 cm^{−1}, and a weak feature at 450 cm^{−1}. Based on computations (*vide infra*), we assign these signals to the P–P stretch, which couples with phenyl-based modes ($\tilde{\nu}_{\text{calc}} = 202, 449, \text{ and } 581 \text{ cm}^{-1}$; Figure S125). Whereas it has been argued^{3b,23b} that neither the P–P bond length nor corresponding stretching frequency (Badger’s and Gordy’s rules) are an accurate measure for the P–P bond’s strength, we note that these values are similar to the ones reported for the diphosphonium dication in [Me₃P–PMe₃][OTf]₂ ($\tilde{\nu} = 207, 456, 692 \text{ cm}^{-1}$; $\tilde{\nu}_{\text{calc}} = 212, 444, 670 \text{ cm}^{-1}$; Figure S126). The cyclovoltammetric analysis in pentafluorobenzene (Figure S110) revealed that dimeric **1** is a potent oxidant with a redox potential of $E = +1.44 \text{ V vs Fc/Fc}^+$, which exceeds that of monomeric PPh₃ ($E = \sim 0.88 \text{ V vs Fc/Fc}^+$) by almost 0.6 V.

Quantum chemical calculations at the density functional theory (DFT) level were performed to understand the stability of 1^{2+} . The topological analysis of the electron density (QTAIM; Scheme 2c) affords a bond critical point (bcp) connecting the two phosphorus atoms. The negative sign of the Laplacian at the bcp ($\nabla^2\rho(r_{\text{bcp}}) = -5.38 \text{ e } \text{Å}^{-5}$) and the

bond order (DI = 0.70) are consistent with a covalent interaction and local charge accumulation, coupled to charge depletion in the area opposed to the P–P bond. The QTAIM descriptors are similar to those reported for [Me₃P–PMe₃]²⁺ ($\rho(r_{\text{bcp}}) = 0.82 \text{ e } \text{Å}^{-3}$; $\nabla^2\rho(r_{\text{bcp}}) = -4.45 \text{ e } \text{Å}^{-5}$), yet enhanced covalency is found for carbon-congener **1** ($\rho(r_{\text{bcp}}) = 1.26 \text{ e } \text{Å}^{-3}$; $\nabla^2\rho(r_{\text{bcp}}) = -10.55 \text{ e } \text{Å}^{-5}$; DI = 0.85). Energy Decomposition Analysis coupled with Natural Orbitals for Chemical Valence (EDA-NOCV³³; Tables S5–S10) was performed to understand the nature of the P–P bond in 1^{2+} in the gas phase and to put it into context with related molecules. The interaction energy in 1^{2+} ($\Delta E_{\text{int}} = -122 \text{ kJ mol}^{-1}$) profits from a high dispersion contribution ($\Delta E_{\text{disp}} = -80 \text{ kJ mol}^{-1}$). Dispersion energy is virtually the same for Ph₃C–CPh₃ ($\Delta E_{\text{disp}} = -81 \text{ kJ mol}^{-1}$; $\Delta E_{\text{int}} = -49 \text{ kJ mol}^{-1}$) despite the difference of the C–C and P–P distances, yet it is smaller for [Me₃P–PMe₃]²⁺ ($\Delta E_{\text{disp}} = -27 \text{ kJ mol}^{-1}$). We note that the electrostatic contribution largely balances with Pauli repulsion (1^{2+} , $\Delta E_{\text{Pauli}} + \Delta E_{\text{elstat}} = (792 - 206) = +586 \text{ kJ mol}^{-1}$; [Me₃P–PMe₃]²⁺, $\Delta E_{\text{Pauli}} + \Delta E_{\text{elstat}} = (543 + 7) = +551 \text{ kJ mol}^{-1}$), just as is the case for the σ -interaction (1^{2+} , $\Delta E_{\text{orb-}\sigma} = -483 \text{ kJ mol}^{-1}$; [Me₃P–PMe₃]²⁺, $\Delta E_{\text{orb-}\sigma} = -486 \text{ kJ mol}^{-1}$).

Hence, the enhanced gas-phase stability of 1^{2+} ($-D_e = -87 \text{ kJ mol}^{-1}$) in respect to [Me₃P–PMe₃]²⁺ ($-D_e = -19 \text{ kJ mol}^{-1}$; $\Delta E_{\text{int}} = -42 \text{ kJ mol}^{-1}$) is essentially due to dispersive stabilization (*vide supra*) as well as collective secondary orbital interactions (Figures S129 and S130) with the phosphines’ substituents (1^{2+} , $\Delta E_{\text{orb-rest}} = -145 \text{ kJ mol}^{-1}$; [Me₃P–PMe₃]²⁺, $\Delta E_{\text{orb-rest}} = -80 \text{ kJ mol}^{-1}$).

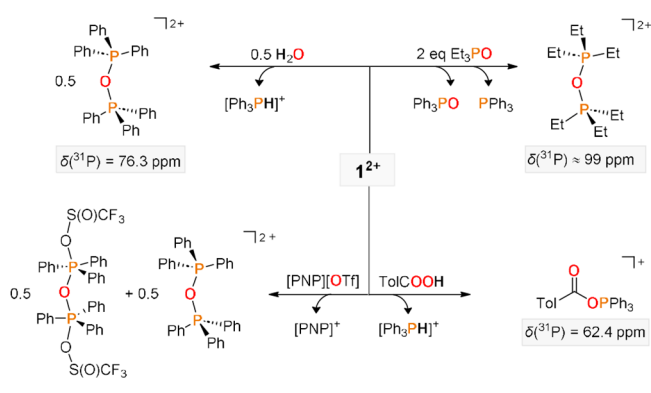
Bickelhaupt and colleagues computationally compared the C–C bond in Ph₃C–CPh₃ with the Si–Si bond in Ph₃Si–SiPh₃.³⁴ As both molecules’ ΔE_{int} values are comparable, it was suggested that the dissociation of Ph₃C–CPh₃ is more facile than that of Ph₃Si–SiPh₃ due to the much higher strain *viz.* preparation energy penalty ($\Delta\Delta E_{\text{prep}} = +267 \text{ kJ mol}^{-1}$).³⁴ The strain energy in 1^{2+} is likewise much smaller ($\Delta E_{\text{prep}} = +34 \text{ kJ mol}^{-1}$) compared to that of Ph₃C–CPh₃ ($\Delta E_{\text{prep}} = +329 \text{ kJ mol}^{-1}$). We thus conclude that the P–P bond in 1^{2+} ($-D_e = -87 \text{ kJ mol}^{-1}$) is weaker than the Si–Si bond in Ph₃Si–SiPh₃ due to electrostatics, but stronger than the C–C bond in Ph₃C–CPh₃ ($-D_e = -49 \text{ kJ mol}^{-1}$) due to the reduced preparation energy. Indeed, [Ph₃N–NPh₃]²⁺ is thermodynamically not stable, as it suffers from both a large preparation energy as well as electrostatic repulsion between two formally cationic charged nitrogen atoms with a short N–N distance (Figure S128). In fact, monocationic [Ph₃P–PPh₂]⁺ and neutral Ph₂P–PPh₂ show only minor changes in the optimized P–P bond lengths with respect to the dication 1^{2+} . However, these compounds feature strong P–P bonds ([Ph₃P–PPh₂]⁺, $-D_e = -309 \text{ kJ mol}^{-1}$; [Ph₂P–PPh₂], $-D_e = -226 \text{ kJ mol}^{-1}$), mostly attributable to more favorable electrostatics ΔE_{elstat} (Table S5).

We furthermore computed the free-energy profile for the formation of Gomberg’s dimer **III** and the corresponding P-congener **V** in fluorobenzene solution (Scheme 2d). Solvation renders the homolytic P–P bond cleavage in 1^{2+} stronger endergonic (**IV**, $\Delta G = +176 \text{ kJ mol}^{-1}$) than in the gas phase, where this reaction is facile (Figure S118; $\Delta G_{\text{gas}} = +33 \text{ kJ mol}^{-1}$). As dearomatization is not coupled to efficient charge-delocalization, addition product **V** is also very high in energy ($\Delta G = +142 \text{ kJ mol}^{-1}$). Opposed to 1^{2+} , solvation does not play a crucial role for the dissociation of neutral **I** into trityl radicals **II** ($\Delta G = -21 \text{ kJ mol}^{-1}$, Figure S119; $\Delta G_{\text{gas}} = -14 \text{ kJ mol}^{-1}$).

mol^{-1} ; Figure S120) and neither for the further transformation to Gombert's dimer **III** ($\Delta G = -9 \text{ kJ mol}^{-1}$, Figure S119; $\Delta G_{\text{gas}} = -5 \text{ kJ mol}^{-1}$, Figure S120), which profits from the generation of a strong $\text{C}=\text{C}$ double bond.

Efforts were conducted to gauge the Lewis-acidity of **1** (Ph_3P^{2+} , respectively),³⁵ as computations predict exceedingly strong *Fluoride Ion Abstraction* ($\text{FIA} = 1237 \text{ kJ mol}^{-1}$; $\text{FIA}_{\text{solv}} = 511 \text{ kJ mol}^{-1}$) capabilities as well as a high *Hydride Ion Affinity* ($\text{HIA} = 1318 \text{ kJ mol}^{-1}$; $\text{HIA}_{\text{solv}} = 574 \text{ kJ mol}^{-1}$; Table S12). Indeed, both the addition of *para*-fluorobenzonitrile³⁶ and triethylphosphine oxide (Gutmann–Beckett method)³⁷ proved unproductive. Dication 1^{2+} adds to nitriles under P–P bond cleavage (*vide infra*) instead of forming stable adducts, whereas triethylphosphine oxide leads to oxygen transfer, thereby generating a stoichiometric mixture of triphenylphosphine oxide, triphenylphosphine, and $[\text{Et}_3\text{P}-\text{O}-\text{PEt}_3]^{2+}$ (Scheme 3).

Scheme 3. Deoxygenation of Et_3PO , Water, *p*-Toluic Acid, and $[\text{PNP}][\text{OTf}]$ by 1^{2+} ; $[\text{Al}^{\text{F}}]$ Anions Are Omitted for Clarity; All Reactions Were Conducted in *o*DFB at Ambient Temperature with Quantitative Conversion upon Mixing



Consequently, we also explored the reaction with other oxygen-containing molecules such as water,¹² a triflate salt, and *p*-toluic acid. The controlled partial hydrolysis cleanly generated the aluminate analogue of Hendrickson's reagent $[(\text{Ph}_3\text{P})_2\text{O}][\text{OTf}]_2$ ("POP")³⁸ and a stoichiometric amount of triphenylphosphonium salt $[\text{Ph}_3\text{PH}]^+$. This reaction is remarkable, as Hendrickson's reagent itself finds use for challenging dehydration reactions.³⁹ In fact, and highlighting exceeding oxophilicity, we observed the abstraction of oxygen atoms upon adding the triflate salt $[\text{PNP}][\text{OTf}]$ ($\text{PNP} = [\text{Ph}_3\text{PNPPh}_3]^+$) to **1**.⁴⁰ The reaction with *p*-toluic acid generated the respective acyloxyphosphonium salt, which serves as the activated mixed-anhydride intermediate in the Appel⁴¹ and Mitsunobu⁴² reactions.

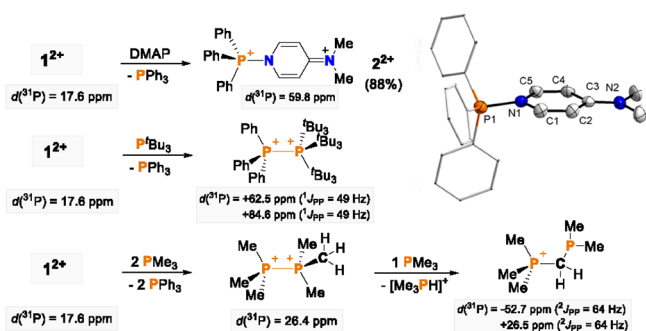
Further detailed reactivity studies were conducted to gauge the interplay of heterolytic *versus* homolytic P–P bond cleavage. Dimethylaminopyridine (DMAP) readily replaces triphenylphosphine in *o*DFB solution at room temperature, thereby generating P(V) and P(III) products under heterolytic P–P bond cleavage (**2**, Scheme 4a). sc-XRD crystallography unambiguously confirmed the structure of **2**,⁴³ where both the P–N (1.719(2) Å) as well as $\text{C}=\text{NMe}_2$ (1.320(4) Å) bond lengths in the solid state are consistent with the values found for $[\text{Me}_3\text{P}(\text{DMAP})][\text{OTf}]_2$ (P–N, 1.720(3); $\text{C}=\text{NMe}_2$ 1.319(4) Å),²⁴ thus indicating pronounced delocalization of cationic charge onto the DMAP substituent. Note that the equilibrium lies in the case of $[\text{Me}_3\text{P}(\text{DMAP})][\text{OTf}]_2$ at the

side of $[\text{Me}_3\text{P}-\text{PMe}_3][\text{OTf}]_2$. The substitution of PPh_3 proceeds according to quantum-chemical calculations barrierless through an $\text{S}_{\text{N}}2$ -type mechanism (Figure S131), thereby highlighting the Lewis acidity of **1**. We analyzed the P–P bond polarization along the reaction coordinate by the occupations of σ -type effective fragment orbitals (EFOs)⁴⁴ of the triphenylphosphine fragments (Figure S132).⁴⁵ DMAP polarizes the P–P bond already at a long distance ($d_{\text{P-N}} = 2.931 \text{ \AA}$), rendering the former 1^{2+} effectively a triphenylphosphine-stabilized triphenylphosphorandiylium dication.

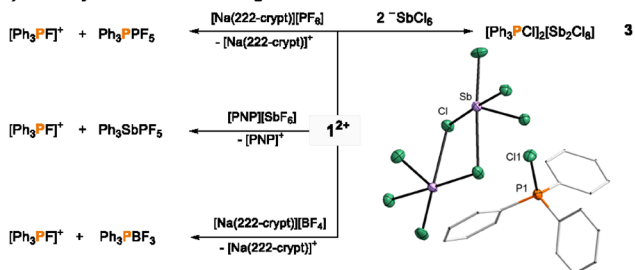
The corresponding substitution reaction to the mixed biscationic diphosphonium dication $[\text{Ph}_3\text{P}-\text{P}^t\text{Bu}_3]^{2+}$ and PPh_3 was obtained in the reaction with P^tBu_3 . The homodimer $[\text{Me}_3\text{P}-\text{PMe}_3]^{2+}$ is formed upon treatment with trimethylphosphine, which (i) indicates that 1^{2+} is a stronger oxidant (less stable, respectively) than $[\text{Me}_3\text{P}-\text{PMe}_3]^{2+}$, and (ii) suggests that dispersion plays a role in the stabilization of $[\text{Ph}_3\text{P}-\text{P}^t\text{Bu}_3]^{2+}$. Running this reaction with overall three equivalents of PMe_3 generated $[\text{Me}_3\text{PH}]^+$ and $[\text{Me}_3\text{PCH}_2\text{PMe}_2]^+$,^{21b,d} hence delineating why $[\text{Me}_3\text{P}-\text{PMe}_3]^{2+}$ is opposed to **1** of moderate synthetic use in the presence of bases. Eventually, salt **1** was found to cleanly generate corresponding halotriphenylphosphonium salts in the halide abstraction reactions with the $^-\text{BF}_4$, $^-\text{PF}_6$, $^-\text{SbCl}_6$, and even $^-\text{SbF}_6$ anions, which commonly serves as a benchmark for Lewis-superacidity (Scheme 4b).^{35c,46}

Compound **1** also engages in formally homolytic P–P bond addition reactions (Scheme 4c). Insertion into the S–S bond was obtained in the reaction with diphenyldisulfide, thereby affording the $[\text{Ph}_3\text{PSPH}]^+$ cations. The transfer of two Ph_3P^+ substituents was also observed in the reaction with unsaturated π -systems, namely, organic nitriles. Keeping **1** at room temperature over 2 days in acetonitrile led to the quantitative conversion to the addition product **Me5**, which was isolated in crystalline form in 23% yield. According to the *in situ* ^{31}P NMR spectroscopic analysis, this reaction involves the tautomerization of intermediate **Me4**. Indeed, **Ph4** was isolated upon reaction with benzonitrile. The addition reaction to nitriles highlights the group-transfer capabilities of 1^{2+} , as electron-deficient nitriles are difficult to activate under oxidative conditions. In fact, related nitrile addition reactions are only known for tungsten(0) complexes⁴⁷ and triphosphiranes,⁴⁸ yet not phosphine derivatives. DFT calculations indicate that the addition to nitriles is only formally homolytic in nature and instead proceeds stepwise via substitution of PPh_3 (Figures S133 and S134).

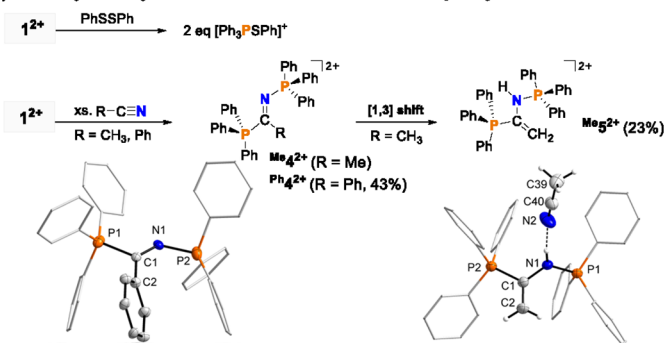
Compound **1** is stable in dichloromethane at room temperature, and EPR is silent, hence indicating that the homolytic P–P bond scission is thermally challenging. However, irradiation in dichloromethane by a xenon lamp afforded the chlorotriphenylphosphonium cation, tentatively suggesting photolytic P–P bond cleavage (Scheme 4d). In *ortho*-difluorobenzene, **1** is stable even upon refluxing overnight, according to the NMR spectroscopic analysis. Again, the irradiation of the sample led to a swift reaction at room temperature, namely, the CH-phosphoranylation of the solvent under the generation of $[\text{Ph}_3\text{PH}]^+$ within 3 h. This formally electrophilic aromatic substitution is unusual, as it proceeds with an electron-deficient arene. It thus prospects synthetically useful substitution reactions with electron-rich arenes. Experimental evidence for homolytic P–P bond photolysis came from irradiation in the presence of 50 equiv of 9,10-dihydroanthracene (DHA; BDFE = 305 kJ mol^{-1}).⁴⁹

Scheme 4. Heterolytic (a, b) and Homolytic (c, d) Bond Cleavage Reactions of **1**; [Al^F] Anions Are Omitted for Clarity^aa) Heterolytic P–P Bond Cleavage Reactions: PPh₃ Substitution

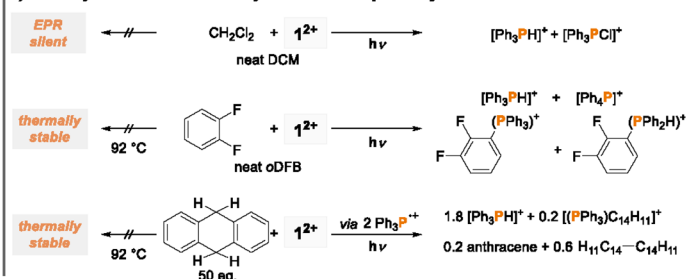
b) Heterolytic P–P Bond Cleavage Reactions: Halide Abstraction



c) Formally Homolytic P–P Bond Addition Reactions: Diphenyl Disulfide and Nitriles



d) Homolytic P–P Bond Photolysis: CH-Phosphoranylation and H-Atom Abstraction



^aAll Reactions were performed in oDFB and proceeded quantitatively. Most hydrogen atoms within crystal structure representations are omitted for clarity, thermal ellipsoids are given at 50% probability. Only one of four independent [PPh₃Cl]⁺ moieties and a symmetry-generated part of the anion in **3** are shown for clarity (see ESI for details). Selected bond lengths [Å] for 2²⁺: P1–N1, 1.719(2); N1–C1, 1.384(4); C1–C2, 1.339(4); C2–C3, 1.423(4); C4–C5, 1.329(4); C3–C4, 1.433(4); C3–N2, 1.320(4). See SI for further metrics.

Quantitative conversion was obtained within less than 30 min, thereby generating [Ph₃PH]⁺ as the major product. Strikingly, the NMR-spectroscopic analysis (Figures S95–100) revealed that anthracene formed substoichiometrically (0.2 equiv), whereas the homocoupled hydroanthracenyl dimer (0.6 equiv) formed majorly. This observation confirms hydroanthracenyl radicals as intermediates and hence a radical H-atom abstraction mechanism.

CONCLUSIONS

We report that the oxidation of triphenylphosphine furnishes the hexaphenyl-1,2-diphosponium dication in the form of its perfluorinated alkoxy aluminate salt **1**. This reaction involves the dimerization of the transient triphenylphosphine radical cation. Highlighting cooperativity, this dimerization boosts the redox-potential by +0.6 V and hence generates a potent oxidant with $E = +1.44$ V vs Fc/Fc⁺, which oxidizes trimethylphosphine. Quantum chemical calculations rationalize that 1²⁺, valence isoelectronic with hexaphenylethane, does not form the equivalent of Gomberg's dimer, as the phosphorus addition product is thermodynamically disfavored. Mimicking halogens, salt **1** may react by both heterolytic and homolytic pathways. Leading to reactivity akin to Frustrated Lewis Pairs (FLPs), heterolytic P–P bond cleavage dominates in the absence of light, hence rendering **1** a surrogate of the triphenylphosphorandiylium dication Ph₃P²⁺. It serves as a precursor for the mixed diphosponium dication [Ph₃P–P^tBu₃]²⁺ and as a superacidic halide- and oxygen-abstraction and/or dehydration reagent. Diphosporanylation of the electron-deficient C≡N multiple bond occurs in the reaction with benzo- and acetonitrile. The irradiation with UV-light induces homolytic P–P bond cleavage to triphenylphosphine radical cations Ph₃P^{•+}, which engage in H-atom abstraction and

arene CH phosphoranylation. In short, compound **1** complements our knowledge on the trityl radical and improves our understanding of oxidation catalysis with ubiquitous triphenylphosphine and corresponding transient triphenylphosphine radical cations. It thereby presents itself as a powerful Lewis acid, oxidant, as well as a powerful H-atom abstraction, deoxygenation, and phosphoranylation agent.

ASSOCIATED CONTENT

Supporting Information

The Supporting Information is available free of charge at <https://pubs.acs.org/doi/10.1021/jacs.5c01271>.

Synthetic procedures, spectroscopic data, computational and crystallographic details (PDF)

Accession Codes

Deposition Numbers 2411876–2411879 and 2430879 contain the supplementary crystallographic data for this paper. These data can be obtained free of charge via the joint Cambridge Crystallographic Data Centre (CCDC) and Fachinformationszentrum Karlsruhe Access Structures service.

AUTHOR INFORMATION

Corresponding Authors

Robert Weiss – Friedrich-Alexander-Universität (FAU) Erlangen-Nürnberg, 91058 Erlangen, Germany; Email: weiss@chemie.uni-erlangen.de

Pedro Salvador – Institut de Química Computacional I Catàlisi, Departament de Química, Universitat de Girona, 17003 Girona, Spain; orcid.org/0000-0003-1823-7295; Email: pedro.salvador@udg.edu

Dominik Munz – Coordination Chemistry, Saarland University, D-66123 Saarbrücken, Germany; orcid.org/

0000-0003-3412-651X; Email: dominik.munz@uni-saarland.de

Authors

Fabian Dankert – Coordination Chemistry, Saarland University, D-66123 Saarbrücken, Germany; orcid.org/0000-0002-6806-4794

Simon P. Muhm – Coordination Chemistry, Saarland University, D-66123 Saarbrücken, Germany

Chandan Nandi – Coordination Chemistry, Saarland University, D-66123 Saarbrücken, Germany

Sergi Danés – Institut de Química Computacional i Catàlisi, Departament de Química, Universitat de Girona, 17003 Girona, Spain; orcid.org/0000-0003-4777-0398

Sneha Mullassery – Coordination Chemistry, Saarland University, D-66123 Saarbrücken, Germany

Petra Herbeck-Engel – INM Leibniz Institute for New Materials, 66123 Saarbrücken, Germany

Bernd Morgenstern – Inorganic Solid-State Chemistry, Saarland University, D-66123 Saarbrücken, Germany

Complete contact information is available at:
<https://pubs.acs.org/10.1021/jacs.5c01271>

Funding

This project has received funding from the European Research Council (ERC) under the European Union's Horizon 2020 Research and Innovation Program (grant no. 948185). B.M. and F.D. thank for the instrumentation and technical assistance for this work, provided by the Service Center X-ray Diffraction, with financial support from Saarland University and the German Science Foundation DFG (project numbers INST 256/506-1 and INST 256/582-1). We gratefully acknowledge scientific support and HPC resources provided by the Erlangen National High Performance Computing Center (NHR@FAU) of the Friedrich-Alexander-Universität (FAU) Erlangen-Nürnberg. We thank the NHR funding provided by federal and Bavarian state authorities. The NHR@FAU hardware is partially funded by the German Research Foundation (DFG)—440719683. P.S. and S.D. acknowledge the Ministerio de Ciencia, Innovación y Universidades (MCIU) grant number PID2022-140666NB-C22.

Notes

The authors declare no competing financial interest.

ACKNOWLEDGMENTS

We thank C. W. M. Kay, G. Kickelbick, and K. Hollemeyer (Servicestelle Massenspektrometrie) for support with EPR, DSC, and HRMS measurements, and I. Krossing, as well as M. Sellin, for helpful discussion.

ABBREVIATIONS

[Al^F], [Al{OC(CF₃)₃}₄]; bcp, bond critical point; BDFE, bond dissociation free energy; DHA, 9,10-dihydroanthracene; DMAP, dimethylaminopyridine; DFT, density functional theory; DHA, dihydroanthracene; EDA-NOCV, energy decomposition analysis with natural orbitals for chemical valence; Fc, ferrocene; FLP, frustrated Lewis pair; IR, infrared; oDFB, 1,2-difluorobenzene; [phen^F]⁺, [perfluoro-5,10-bis-(perfluorophenyl)-5,10-dihydrophenazinium]⁺; PFB, pentafluorobenzene; NMR, nuclear magnetic resonance; QTAIM, quantum theory of atoms in molecules; sc-XRD, single-crystal X-ray diffractometry; TFB, 1,2,3,4-tetrafluorobenzene

REFERENCES

- (1) (a) Gomberg, M. An instance of trivalent carbon: triphenylmethyl. *J. Am. Chem. Soc.* **1900**, *22*, 757–771. (b) Gomberg, M. Triphenylmethyl, ein Fall von dreiwertigem Kohlenstoff. *Ber. Dtsch. Chem. Ges.* **1900**, *33*, 3150–3163.
- (2) Lankamp, H.; Nauta, W. T.; MacLean, C. A new interpretation of the monomer-dimer equilibrium of triphenylmethyl- and alkylsubstituted-diphenyl methyl-radicals in solution. *Tetrahedron Lett.* **1968**, *9*, 249–254.
- (3) (a) Schlenk, W.; Renning, J.; Racky, G. Über das Hexaphenylsilicoäthan und einige Biphenyl-Substitutionsprodukte des gewöhnlichen Äthans und Äthylens. *Ber. Dtsch. Chem. Ges.* **1911**, *44*, 1178–1182. (b) Rummel, L.; Schümann, J. M.; Schreiner, P. R. Hexaphenylditretels—When Longer Bonds Provide Higher Stability. *Chem.—Eur. J.* **2021**, *27*, 13699–13702.
- (4) Eisch, J. J.; Dluzniewski, T.; Behrooz, M. The nature of Krause's adducts: The structure of the 1:1 adduct of triphenylborane with sodium metal. *Heteroat. Chem.* **1993**, *4*, 235–241.
- (5) (a) Seo, E. T.; Nelson, R. F.; Fritsch, J. M.; Marcoux, L. S.; Leedy, D. W.; Adams, R. N. Anodic Oxidation Pathways of Aromatic Amines. Electrochemical and Electron Paramagnetic Resonance Studies. *J. Am. Chem. Soc.* **1966**, *88*, 3498–3503. (b) Marcoux, L. S.; Adams, R. N.; Feldberg, S. W. Dimerization of Triphenylamine Cation Radicals. Evaluation of Kinetics Using the Rotating Disk Electrode. *J. Phys. Chem.* **1969**, *73*, 2611–2614.
- (6) (a) Stein, M.; Winter, W.; Rieker, A. Hexakis(2,6-di-tert-butyl-4-biphenyl)ethane—The First Unbridged Hexaarylethane. *Angew. Chem. Int. Ed.* **1978**, *17*, 692–694. (b) Grimme, S.; Schreiner, P. R. Steric Crowding Can Stabilize a Labile Molecule: Solving the Hexaphenylethane Riddle. *Angew. Chem. Int. Ed.* **2011**, *50*, 12639–12642. (c) Uchimura, Y.; Takeda, T.; Katoono, R.; Fujiwara, K.; Suzuki, T. New Insights into the Hexaphenylethane Riddle: Formation of an α , α -Dimer. *Angew. Chem. Int. Ed.* **2015**, *54*, 4010–4013. (d) Rösel, S.; Balestrieri, C.; Schreiner, P. R. Sizing the role of London dispersion in the dissociation of all-meta tert-butyl hexaphenylethane. *Chem. Sci.* **2017**, *8*, 405–410. (e) Rösel, S.; Becker, J.; Allen, W. D.; Schreiner, P. R. Probing the Delicate Balance between Pauli Repulsion and London Dispersion with Triphenylmethyl Derivatives. *J. Am. Chem. Soc.* **2018**, *140*, 14421–14432.
- (7) (a) Vasilevska, A.; Slanina, T. Structure–property–function relationships of stabilized and persistent C- and N-based triaryl radicals. *Chem. Commun.* **2024**, *60*, 252–264. (b) Heuer, A. M.; Coste, S. C.; Singh, G.; Mercado, B. Q.; Mayer, J. M. A Guide to Tris(4-Substituted)-triphenylmethyl Radicals. *J. Org. Chem.* **2023**, *88*, 9893–9901.
- (8) Li, S.; Shiri, F.; Xu, G.; Yiu, S.-M.; Lee, H. K.; Ng, T. H.; Lin, Z.; Lu, Z. Reactivity of a Hexaaryldiboron(6) Dianion as Boryl Radical Anions. *J. Am. Chem. Soc.* **2024**, *146*, 17348–17354.
- (9) Bidan, G.; Genies, M. Addition du cation triphenylmethyl sur le triphenylphosphane. Mécanisme d'isomérisation du cation trityltriphenylphosphane. *Tetrahedron Lett.* **1978**, *19*, 2499–2502.
- (10) (a) Powell, R. L.; Hall, C. D. Phosphinium radical cation. *J. Am. Chem. Soc.* **1969**, *91*, 5403–5404. (b) Reichl, K. D.; Ess, D. H.; Radosevich, A. T. Catalyzing Pyramidal Inversion: Configurational Lability of P-Stereogenic Phosphines via Single Electron Oxidation. *J. Am. Chem. Soc.* **2013**, *135*, 9354–9357. (c) Yasui, S.; Tojo, S.; Majima, T. Reaction of Triarylphosphine Radical Cations Generated from Photoinduced Electron Transfer in the Presence of Oxygen. *J. Org. Chem.* **2005**, *70*, 1276–1280.
- (11) (a) Schiavon, G.; Zecchin, S.; Cogoni, G.; Bontempelli, G. Anodic oxidation of triphenylphosphine at a platinum electrode in acetonitrile medium. *J. Electroanal. Chem. Interface Electrochem.* **1973**, *48*, 425–431. (b) Leca, D.; Fensterbank, L.; Lacôte, E.; Malacria, M. Recent advances in the use of phosphorus-centered radicals in organic chemistry. *Chem. Soc. Rev.* **2005**, *34*, 858–865. (c) Luo, K.; Yang, W.-C.; Wu, L. Photoredox Catalysis in Organophosphorus Chemistry. *Asian J. Org. Chem.* **2017**, *6*, 350–367. (d) Rossi-Ashton, J. A.; Clarke, A. K.; Unsworth, W. P.; Taylor, R. J. K. Phosphoranyl Radical Fragmentation Reactions Driven by Photoredox Catalysis. *ACS Catal.*

- 2020, 10, 7250–7261. (e) Hu, X.-Q.; Hou, Y.-X.; Liu, Z.-K.; Gao, Y. Recent advances in phosphoranyl radical-mediated deoxygenative functionalisation. *Org. Chem. Front.* **2020**, 7, 2319–2324. (f) Pan, D.; Nie, G.; Jiang, S.; Li, T.; Jin, Z. Radical reactions promoted by trivalent tertiary phosphines. *Org. Chem. Front.* **2020**, 7, 2349–2371. (g) Roediger, S.; Le Saux, E.; Boehm, P.; Morandi, B. Coupling of unactivated alkyl electrophiles using frustrated ion pairs. *Nature* **2024**, 636, 108–114.
- (12) Zhang, J.; Mück-Lichtenfeld, C.; Studer, A. Photocatalytic phosphine-mediated water activation for radical hydrogenation. *Nature* **2023**, 619, 506–513.
- (13) (a) Pan, X.; Chen, X.; Li, T.; Li, Y.; Wang, X. Isolation and X-ray Crystal Structures of Triarylphosphine Radical Cations. *J. Am. Chem. Soc.* **2013**, 135, 3414–3417. (b) Menard, G.; Hatnean, J. A.; Cowley, H. J.; Lough, A. J.; Rawson, J. M.; Stephan, D. W. C-H bond activation by radical ion pairs derived from $R_3P/Al(C_6F_5)_3$ frustrated Lewis pairs and N_2O . *J. Am. Chem. Soc.* **2013**, 135, 6446–6449. (c) Liu, L.; Cao, L. L.; Shao, Y.; Ménard, G.; Stephan, D. W. A Radical Mechanism for Frustrated Lewis Pair Reactivity. *Chem.* **2017**, 3, 259–267. (d) Holtrop, F.; Jupp, A. R.; Kooij, B. J.; van Leest, N. P.; de Bruin, B.; Slootweg, J. C. Single-Electron Transfer in Frustrated Lewis Pair Chemistry. *Angew. Chem. Int. Ed.* **2020**, 59, 22210–22216. (e) Das, B.; Makol, A.; Kundu, S. Phosphorus radicals and radical ions. *Dalton Trans.* **2022**, 51, 12404–12426.
- (14) (a) Stephan, D. W.; Erker, G. Frustrated Lewis Pair Chemistry: Development and Perspectives. *Angew. Chem. Int. Ed.* **2015**, 54, 6400–6441. (b) Stephan, D. W. The broadening reach of frustrated Lewis pair chemistry. *Science* **2016**, 354, No. aaf7229.
- (15) (a) Jupp, A. R.; Stephan, D. W. New Directions for Frustrated Lewis Pair Chemistry. *Trends Chem.* **2019**, 1, 35–48. (b) Ju, M.; Lu, Z.; Novaes, L. F. T.; Martinez Alvarado, J. I.; Lin, S. Frustrated Radical Pairs in Organic Synthesis. *J. Am. Chem. Soc.* **2023**, 145, 19478–19489. (c) van der Zee, L. J. C.; Pahar, S.; Richards, E.; Melen, R. L.; Slootweg, J. C. Insights into Single-Electron-Transfer Processes in Frustrated Lewis Pair Chemistry and Related Donor–Acceptor Systems in Main Group Chemistry. *Chem. Rev.* **2023**, 123, 9653–9675.
- (16) Ham, G.; Kim, Y.; Jang, W.-D.; Kim, S. An Isolable Triarylphosphine Radical Cation Electronically Stabilized by Through-Space Radical Delocalization. *J. Am. Chem. Soc.* **2024**, 146, 31405–31411.
- (17) Makovetskii, Y. P.; Feshchenko, N. G. Chemical Properties of Hexaalkylbisphosphonium Bistriiodides. *Zh. Obshch. Khim.* **1985**, 55, 1003–1006.
- (18) Weigand, J. J.; Riegel, S. D.; Burford, N.; Decken, A. Prototypical Phosphorus Analogues of Ethane: General and Versatile Synthetic Approaches to Hexaalkylated P-P Diphosphonium Cations. *J. Am. Chem. Soc.* **2007**, 129, 7969–7976.
- (19) Nikitin, E. V.; Romakhin, A. S.; Zagumennov, V. A.; Babkin, Y. A. Electrochemical synthesis of diphosphonium salts, their reactivity and role in organic electrosynthesis. *Electrochim. Acta* **1997**, 42, 2217–2224.
- (20) Siddique, R. M.; Winfield, J. M. The oxidation of dimethyl sulphide, trimethylamine, and trimethylphosphine by solvated copper(II) or thallium(III) hexafluorometallates in acetonitrile. *Can. J. Chem.* **1989**, 67, 1780–1784.
- (21) (a) Dyker, C. A.; Burford, N. catena-Phosphorus Cations. *Chem.—Asian J.* **2008**, 3, 28–36. (b) Robertson, A. P. M.; Chitnis, S. S.; Jenkins, H. A.; McDonald, R.; Ferguson, M. J.; Burford, N. Establishing the Coordination Chemistry of Antimony(V) Cations: Systematic Assessment of $Ph_4Sb(OTf)$ and $Ph_3Sb(OTf)_2$ as Lewis Acceptors. *Chem.—Eur. J.* **2015**, 21, 7902–7913. (c) Chitnis, S. S.; Robertson, A. P. M.; Burford, N.; Patrick, B. O.; McDonald, R.; Ferguson, M. J. Bipyridine complexes of E^{3+} ($E = P, As, Sb, Bi$): strong Lewis acids, sources of $E(OTf)_3$ and synthons for EI and EV cations. *Chem. Sci.* **2015**, 6, 6545–6555. (d) Chitnis, S. S.; Robertson, A. P. M.; Burford, N.; Weigand, J. J.; Fischer, R. Synthesis and reactivity of cyclo-tetra(stibinophosphonium) tetracations: redox and coordination chemistry of phosphine–antimony complexes. *Chem. Sci.* **2015**, 6, 2559–2574. (e) Robertson, A. P. M.; Burford, N.; McDonald, R.; Ferguson, M. J. Coordination Complexes of Ph_3Sb^{2+} and Ph_3Bi^{2+} : Beyond Pnictonium Cations. *Angew. Chem. Int. Ed.* **2014**, 53, 3480–3483.
- (22) Munz, D.; Meyer, K. Charge frustration as a concept for ligand design and functional group transfer. *Nat. Rev. Chem.* **2021**, 5, 422–439.
- (23) (a) Wolstenholme, D. J.; Weigand, J. J.; Davidson, R. J.; Pearson, J. K.; Cameron, T. S. Understanding the Electronic Structure, Reactivity, and Hydrogen Bonding for a 1,2-Diphosphonium Dication. *J. Phys. Chem. A* **2008**, 112, 3424–3431. (b) Chitnis, S. S.; Whalen, J. M.; Burford, N. Influence of charge and coordination number on bond dissociation energies, distances, and vibrational frequencies for the phosphorus–phosphorus bond. *J. Am. Chem. Soc.* **2014**, 136, 12498–12506.
- (24) Weigand, J. J.; Burford, N.; Decken, A.; Schulz, A. Preparation and Characterization of a Ligand-Stabilized Trimethylphosphane Dication. *Eur. J. Inorg. Chem.* **2007**, 2007, 4868–4872.
- (25) Holthausen, M. H.; Bayne, J. M.; Mallov, I.; Dobrovetsky, R.; Stephan, D. W. 1,2-Diphosphonium Dication: A Strong P-Based Lewis Acid in Frustrated Lewis Pair (FLP)-Activations of B–H, Si–H, C–H, and H–H Bonds. *J. Am. Chem. Soc.* **2015**, 137, 7298–7301.
- (26) (a) Caputo, C. B.; Hounjet, L. J.; Dobrovetsky, R.; Stephan, D. W. Lewis Acidity of Organofluorophosphonium Salts: Hydrodefluorination by a Saturated Acceptor. *Science* **2013**, 341, 1374–1377. (b) Bayne, J. M.; Stephan, D. W. Phosphorus Lewis acids: emerging reactivity and applications in catalysis. *Chem. Soc. Rev.* **2016**, 45, 765–774. (c) Burford, N.; Ragogna, P. J. New synthetic opportunities using Lewis acidic phosphines. *J. Chem. Soc., Dalton Trans.* **2002**, 4307–4315.
- (27) (a) Zhou, J.; Liu, L. L.; Cao, L. L.; Stephan, D. W. A Phosphorus Lewis Super Acid: eta5-Pentamethylcyclopentadienyl Phosphorus Dication. *Chem.* **2018**, 4, 2699–2708. (b) Mehlmann, P.; Witteler, T.; Wilm, L. F. B.; Dielmann, F. Isolation, characterization and reactivity of three-coordinate phosphorus dications isoelectronic to alanes and silylium cations. *Nat. Chem.* **2019**, 11, 1139–1143. (c) Waked, A. E.; Chitnis, S. S.; Stephan, D. W. P(v) dications: carbon-based Lewis acid initiators for hydrodefluorination. *Chem. Commun.* **2019**, 55, 8971–8974. (d) Chitnis, S. S.; LaFortune, J. H. W.; Cummings, H.; Liu, L. L.; Andrews, R.; Stephan, D. W. Phosphorus Coordination Chemistry in Catalysis: Air Stable P(III)-Dications as Lewis Acid Catalysts for the Allylation of C–F Bonds. *Organometallics* **2018**, 37, 4540–4544. (e) Humphries, A. L.; Tellier, G. A.; Smith, M. D.; Chianese, A. R.; Peryshkov, D. V. N–H Bond Activation of Ammonia by a Redox-Active Carboranyl Diphosphine. *J. Am. Chem. Soc.* **2024**, 146, 33159–33162.
- (28) (a) Dunn, N. L.; Ha, M.; Radosevich, A. T. Main Group Redox Catalysis: Reversible P^{III}/P^V Redox Cycling at a Phosphorus Platform. *J. Am. Chem. Soc.* **2012**, 134, 11330–11333. (b) Volodarsky, S.; Dobrovetsky, R. Amphiphilic geometrically constrained phosphonium cation. *Chem. Commun.* **2018**, 54, 6931–6934. (c) Wünsche, M. A.; Witteler, T.; Dielmann, F. Lewis Base Free Oxophosphonium Ions: Tunable, Trigonal-Planar Lewis Acids. *Angew. Chem. Int. Ed.* **2018**, 57, 7234–7239. (d) Roth, D.; Stirn, J.; Stephan, D. W.; Greb, L. Lewis Superacid Catecholato Phosphonium Ions: Phosphorus–Ligand Cooperative C–H Bond Activation. *J. Am. Chem. Soc.* **2021**, 143, 15845–15851. (e) Olaru, M.; Mebs, S.; Beckmann, J. Cationic Carbene Analogues: Donor-Free Phosphenium and Arsenium Ions. *Angew. Chem. Int. Ed.* **2021**, 60, 19133–19138. (f) Abbenseth, J.; Townrow, O. P. E.; Goicoechea, J. M. Thermoneutral N–H Bond Activation of Ammonia by a Geometrically Constrained Phosphine. *Angew. Chem. Int. Ed.* **2021**, 60, 23625–23629. (g) Volodarsky, S.; Bawari, D.; Dobrovetsky, R. Dual Reactivity of a Geometrically Constrained Phosphenium Cation. *Angew. Chem. Int. Ed.* **2022**, 61, No. e202208401. (h) Bawari, D.; Toami, D.; Jaiswal, K.; Dobrovetsky, R. Hydrogen splitting at a single phosphorus centre and its use for hydrogenation. *Nat. Chem.* **2024**, 16, 1261–1266.
- (29) (a) Abbenseth, J.; Goicoechea, J. M. Recent developments in the chemistry of non-trigonal pnicogen pincer compounds: from

bonding to catalysis. *Chem. Sci.* **2020**, *11*, 9728–9740. (b) Lipshultz, J. M.; Li, G.; Radosevich, A. T. Main Group Redox Catalysis of Organopnictogens: Vertical Periodic Trends and Emerging Opportunities in Group 15. *J. Am. Chem. Soc.* **2021**, *143*, 1699–1721.

(30) (a) Loh, Y. K.; Melaimi, M.; Gembicky, M.; Munz, D.; Bertrand, G. A crystalline doubly oxidized carbene. *Nature* **2023**, *623*, 66–70. (b) Gong, Y.; Langwald, J.; Mulks, F. F. On the road to isolable geminal carbocations. *Chem.* **2024**, *10*, 3294–3308.

(31) (a) Schorpp, M.; Heizmann, T.; Schmucker, M.; Rein, S.; Weber, S.; Krossing, I. Synthesis and Application of a Perfluorinated Ammonium Radical Cation as a Very Strong Deelectronator. *Angew. Chem. Int. Ed.* **2020**, *59*, 9453–9459. (b) Sellin, M.; Friedmann, C.; Mayländer, M.; Richert, S.; Krossing, I. Towards clustered carbonyl cations $[M_3(CO)_{14}]^{2+}$ (M = Ru, Os): the need for innocent deelectronation. *Chem. Sci.* **2022**, *13*, 9147–9158. (c) Rall, J. M.; Schorpp, M.; Keilwerth, M.; Mayländer, M.; Friedmann, C.; Daub, M.; Richert, S.; Meyer, K.; Krossing, I. Synthesis and Characterization of Stable Iron Pentacarbonyl Radical Cation Salts. *Angew. Chem., Int. Ed.* **2022**, *61*, No. e202204080. (d) Armbruster, C.; Sellin, M.; Seiler, M.; Würz, T.; Oesten, F.; Schmucker, M.; Sterbak, T.; Fischer, J.; Radtke, V.; Hunger, J.; Krossing, I. Pushing redox potentials to highly positive values using inert fluorobenzenes and weakly coordinating anions. *Nat. Commun.* **2024**, *15*, 6721. (e) Sellin, M.; Willrett, J.; Röhner, D.; Heizmann, T.; Fischer, J.; Seiler, M.; Holzmann, C.; Engesser, T. A.; Radtke, V.; Krossing, I. Utilizing the Perfluoronaphthalene Radical Cation as a Selective Deelectronator to Access a Variety of Strongly Oxidizing Reactive Cations. *Angew. Chem., Int. Ed.* **2024**, *63*, No. e202406742.

(32) Engesser, T. A.; Lichtenthaler, M. R.; Schleep, M.; Krossing, I. Reactive p-block cations stabilized by weakly coordinating anions. *Chem. Soc. Rev.* **2016**, *45*, 789–899.

(33) Mitoraj, M. P.; Michalak, A.; Ziegler, T. A Combined Charge and Energy Decomposition Scheme for Bond Analysis. *J. Chem. Theory Comput.* **2009**, *5*, 962–975.

(34) Rodrigues Silva, D.; Blokker, E.; van der Schuur, J. M.; Hamlin, T. A.; Bickelhaupt, F. M. Nature and strength of group-14 A–A' bonds. *Chem. Sci.* **2024**, *15*, 1648–1656.

(35) (a) Greb, L. Lewis Superacids: Classifications, Candidates, and Applications. *Chem.—Eur. J.* **2018**, *24*, 17881–17896. (b) Erdmann, P.; Schmitt, M.; Sigmund, L. M.; Krämer, F.; Breher, F.; Greb, L. How to Deal with Charge in the Ranking of Lewis Acidity: Critical Evaluation of an Extensive Set of Cationic Lewis Acids. *Angew. Chem., Int. Ed.* **2024**, *63*, No. e202403356. (c) Erdmann, P.; Greb, L. Multidimensional Lewis Acidity: A Consistent Data Set of Chloride, Hydride, Methide, Water and Ammonia Affinities for 183 p-Block Element Lewis Acids. *ChemPhysChem* **2021**, *22*, 935–943.

(36) Kunzler, S.; Rathjen, S.; Merk, A.; Schmidtman, M.; Muller, T. An Experimental Acidity Scale for Intramolecularly Stabilized Silyl Lewis Acids. *Chem.* **2019**, *25*, 15123–15130.

(37) (a) Mayer, U.; Gutmann, V.; Gerger, W. The acceptor number — A quantitative empirical parameter for the electrophilic properties of solvents. *Monatsh. Chem.* **1975**, *106*, 1235–1257. (b) Beckett, M. A.; Strickland, G. C.; Holland, J. R.; Sukumar Varma, K. A convenient n.m.r. method for the measurement of Lewis acidity at boron centres: correlation of reaction rates of Lewis acid initiated epoxide polymerizations with Lewis acidity. *Polymer* **1996**, *37*, 4629–4631. (c) Erdmann, P.; Greb, L. What Distinguishes the Strength and the Effect of a Lewis Acid: Analysis of the Gutmann–Beckett Method. *Angew. Chem., Int. Ed.* **2022**, *61*, No. e202114550.

(38) Hendrickson, J. B.; Schwartzman, S. M. Triphenyl phosphine ditriflate: A general oxygen activator. *Tetrahedron Lett.* **1975**, *16*, 277–280.

(39) Hendrickson, J. B.; Mistry, S. N.; Moussa, Z.; Al-Masri, H. T., Triphenylphosphonium Anhydride Trifluoromethanesulfonate. In *Encyclopedia of Reagents for Organic Synthesis*; Wiley, 2014.

(40) Moussa, Z.; Ahmed, S. A.; ElDouhaibi, A. S.; Al-Raqa, S. Y. NMR Studies and electrophilic properties of triphenylphosphine-trifluoromethanesulfonic anhydride; a remarkable dehydrating reagent

system for the conversion of aldoximes into nitriles. *Tetrahedron Lett.* **2010**, *51*, 1826–1831.

(41) Appel, R. Tertiary Phosphane/Tetrachloromethane, a Versatile Reagent for Chlorination, Dehydration, and P–N Linkage. *Angew. Chem. Int. Ed.* **1975**, *14*, 801–811.

(42) Swamy, K. C. K.; Kumar, N. N. B.; Balaraman, E.; Kumar, K. V. P. Mitsunobu and Related Reactions: Advances and Applications. *Chem. Rev.* **2009**, *109*, 2551–2651.

(43) Pell, T. P.; Couchman, S. A.; Ibrahim, S.; Wilson, D. J. D.; Smith, B. J.; Barnard, P. J.; Dutton, J. L. Diverse Reactions of $PhI(OTf)_2$ with Common 2-Electron Ligands: Complex Formation, Oxidation, and Oxidative Coupling. *Inorg. Chem.* **2012**, *51*, 13034–13040.

(44) Mayer, I. Atomic Orbitals from Molecular Wave Functions: The Effective Minimal Basis. *J. Phys. Chem.* **1996**, *100*, 6249–6257.

(45) Gimferrer, M.; Danés, S.; Andrada, D. M.; Salvador, P. Unveiling the Electronic Structure of the Bi(+1)/Bi(+3) Redox Couple on NCN and NNN Pincer Complexes. *Inorg. Chem.* **2021**, *60*, 17657–17668.

(46) Erdmann, P.; Leitner, J.; Schwarz, J.; Greb, L. An Extensive Set of Accurate Fluoride Ion Affinities for p-Block Element Lewis Acids and Basic Design Principles for Strong Fluoride Ion Acceptors. *ChemPhysChem* **2020**, *21*, 987–994.

(47) (a) Hoffmann, N.; Wismach, C.; Jones, P. G.; Streubel, R.; Huy, N. H. T.; Mathey, F. Synthesis of the first 1,2,3,4-azatriphospholene complex. *Chem. Commun.* **2002**, 454–455.

(b) Burck, S.; Gudat, D.; Nieger, M. Metal-Assisted, Reversible Phosphinyl Phosphination of the Carbon–Nitrogen Triple Bond in a Nitrile. *Angew. Chem. Int. Ed.* **2007**, *46*, 2919–2922.

(48) Chitnis, S. S.; Sparkes, H. A.; Annibale, V. T.; Pridmore, N. E.; Oliver, A. M.; Manners, I. Addition of a Cyclophosphine to Nitriles: An Inorganic Click Reaction Featuring Protio, Organo, and Main-Group Catalysis. *Angew. Chem. Int. Ed.* **2017**, *56*, 9536–9540.

(49) Agarwal, R. G.; Coste, S. C.; Groff, B. D.; Heuer, A. M.; Noh, H.; Parada, G. A.; Wise, C. F.; Nichols, E. M.; Warren, J. J.; Mayer, J. M. Free Energies of Proton-Coupled Electron Transfer Reagents and Their Applications. *Chem. Rev.* **2022**, *122*, 1–49.



CAS BIOFINDER DISCOVERY PLATFORM™

STOP DIGGING THROUGH DATA —START MAKING DISCOVERIES

CAS BioFinder helps you find the
right biological insights in seconds

Start your search

